Mathematical Biosciences and Engineering

http://www.aimspress.com/journal/MBE

MBE, 17(4): 3567–3581
DOI: 10.3934/mbe.2020201
Received: 18 March 2020
Accepted: 7 May 2020
Published: 12 May 2020

Research article

Analysis of dynamic properties on forest restoration-population pressure model

Mingzhu Qu[1], **Chunrui Zhang**[1] **and Xingjian Wang**[2,*]

[1] Department of Mathematics, Northeast Forestry University, Harbin 150040, China
[2] College of Information and Computer Engineering, Northeast Forestry University, Harbin 150040, China

* **Correspondence:** E-mail: jianxingwang@126.com.

Abstract: On the basis of logistic models of forest restoration, we consider the influence of population pressure on forest restoration and establish a reaction diffusion model with Holling II functional responses. We study this reaction diffusion model under Dirichlet boundary conditions and obtain a positive equilibrium. In the square region, we analyze the existence of Turing instability and Hopf bifurcation near this point. The square patterns and mixed patterns are obtained when steady-state bifurcation occurs, the hyperhexagonal patterns appears in Hopf bifurcation.

Keywords: forest restoration; population pressure; Turing instability; Hopf bifurcation; patterns

1. Introduction

Forest is the main part of the whole terrestrial ecosystem. The generation and distribution of interspecies models play an important role in ecological protection and biochemical response. One of the typical models is forest restoration model [1–6]. Many mathematicians and biologists have been paying close attention to these kinds of models since the 1960s.

Okubo [7] defined the process of diffusion as a set of particles, which may be a molecule or a living, through the individual's random movement in space and time. The diffusion models had been widely used in the fields of chemistry, physics and ecology [8]. Diffusion models had also been successfully applied to describe land cover change. Jesse [9] and Svirezhev [10] indicated that when combining reaction terms, these diffusion models became particularly suitable for simulating land use and land cover change because they took into account the dynamics of spatial structure and land cover class. Acevedo et al. [11] described a quantitative model of forest restoration based on diffusion logistic growth (DLG), which provided a new method for study of forest restoration. While considering spatial dependence, the relationship between continuous space and time of forest

restoration is studied. Holmes et al. [12] pointed out that application of DLG model in forest restoration assumed land-cover change could be described as traveling waves diffusing from source to outside at constant rate. It is assumed that tree colonization can be regarded as a small scale forest restoration process and spread irregularly in space.

Recently, land-use and land-cover change (LUCC) had a wide range of impacts on biodiversity, climate and ecosystem services. In Vitousek, Nunes et al. and Houet et al. [13–15], the authors believed that LUCC was the most vital human change on earth. Pereira et al. [16] said it would straightly affect biodiversity. In [17,18], the authors thought the climate was also affected by LUCC. Lambin et al. [19] noted that although LUCC described usual land cover change, most studies payed a lot of attentions to large-scale deforestation processes used by humans, such as agriculture. Forest restoration is becoming more and more common in agricultural intensification processes, especially in the tropics [20–22].

Human activity is one of the main factors leading to change of natural environment. The contradiction between population and forest resources is becoming more and more prominent, so it is important to establish forest restoration-population pressure model to consider the balance between population growth and forest resources.

The objective of this paper is to analyse dynamic properties of forest restoration-population pressure model. In the second section, we establish the population pressure reaction diffusion model under Dirichlet boundary conditions according to the idea [23,24]. And we study the local stability of positive equilibrium of the model in the third section. In the fourth section, the existence conditions of Turing instability and Hopf bifurcation are given in Theorem 4.1 and 4.2, respectively. We obtain two kinds of steady-state bifurcation types, that is, simple bifurcation and double bifurcation. At the same time, we select some values for the parameters, and get numerical simulations to support the results in section 4.

2. Construction of forest restoration-population pressure model

In the classical applications of partial differential equation models to population ecology, organisms are assumed to have Brownian random dispersion, the rate of which is invariant in time and space

$$\frac{\partial u(x,y,t)}{\partial t} = D\left(\frac{\partial^2 u}{\partial x^2} + \frac{\partial^2 u}{\partial y^2}\right),$$

where $u(x, y, t)$ is the density of organisms at spatial coordinates x, y, and time t, and D is the diffusion coefficient that measures dispersal rate.

Holmes et al. [12] pointed out that the diffusion logistic growth (DLG) model is an extension of two-dimensional Fisher Eq [25]. DLG consists of two parts: Brownian random dispersion and logistic population growth. This model can be represented by a partial differential equation:

$$\frac{\partial u}{\partial t} = D_u\left(\frac{\partial^2 u}{\partial x^2} + \frac{\partial^2 u}{\partial y^2}\right) + r_u u\left(1 - \frac{u}{K_u}\right), \tag{2.1}$$

where u stands for forest radio, t for time, D_u for diffusion rate, x and y for spatial position, r_u for natural growth rate, K_u for bearing capacity.

In order to complete the model, we must specify the initial values and boundary conditions. The forest ratio in region $R = \left\{(x, y) \middle| 0 \le x \le L_x, 0 \le y \le L_y \right\}$ is defined as initial value at time $t = 0$,where L_x and L_y represent landscape range of the x and y axes. At the same time, we apply Dirichlet boundary $u = 0$ on the boundary of R, ∂R:

$$\partial R = \begin{cases} (0, y), & 0 \le y \le L_y \\ (L_x, y), & 0 \le y \le L_y \\ (x, 0), & 0 \le x \le L_x \\ \left(x, L_y\right), & 0 \le x \le L_x \end{cases}$$

The current application of the model includes three parameters: diffusion rate (D_u), endogenous growth rate (r_u) and carrying capacity (K_u). The diffusion rate describes rate of change of land cover radio. In the case of land cover change, intrinsic growth rate describes the rate of change of land cover category. Proportion of this land cover category can be increased to the maximum, that is, carrying capacity ($K_u = 1$).

With regard to influence of population on forest resources, we use predator-prey systems for reference and describe the relationship between population and forest as Holling II functional responses [26]. According to [27] and based on Eq (2.1), forest restoration model is considered under population pressure, and the following model is established:

$$\begin{cases} \dfrac{\partial u}{\partial t} = D_u \left(\dfrac{\partial^2 u}{\partial x^2} + \dfrac{\partial^2 u}{\partial y^2} \right) + r_u u \left(1 - \dfrac{u}{K_u} \right) - \dfrac{\beta u}{1 + au} v, \\ \dfrac{\partial v}{\partial t} = D_v \left(\dfrac{\partial^2 v}{\partial x^2} + \dfrac{\partial^2 v}{\partial y^2} \right) + r_v v \left(1 - \dfrac{v}{K_v} \right) + \dfrac{\alpha u}{1 + au} v, \end{cases} \tag{2.2}$$

where v is the population density, a is the half-saturation constant, $\alpha = c\beta$, c is the conversion coefficiency of the population. The term $\beta u / (1 + au)$ denotes the functional response of the population, all parameters are assumed to be positive.

We specify the value of solution of the differential equation at the boundary, then for all $t \ge 0$, the system complies with homogeneous Dirichlet boundary conditions

$$u(x, y, t) = u_0, v(x, y, t) = v_0, (x, y) \in \partial\Omega,$$

where u and v are state variables, (u_0, v_0) is a uniform steady-state solution which is independent of variables, t, x, y and satisfies

$$f(u_0, v_0, \alpha) = g(u_0, v_0, \alpha) = 0.$$

For convenience of calculation, we have recorded D_u, D_N, r_u, r_v and $1/K_u$, $1/K_v$ as d_1, d_2, r_1, r_2 and P, Q, respectively. Therefore, we can obtain

$$\begin{cases} \dfrac{\partial u}{\partial t} = d_1 \Delta u + r_1 u (1 - Pu) - \dfrac{\beta u v}{1 + au}, \\ \dfrac{\partial v}{\partial t} = d_2 \Delta v + r_2 v (1 - Qv) + \dfrac{\alpha u v}{1 + au}. \end{cases} \tag{2.3}$$

3. Linear stability analysis

Consider

$$\begin{cases} r_1 u\,(1 - Pu) - \dfrac{\beta uv}{1 + au} = 0, \\ r_2 v\,(1 - Qv) + \dfrac{\alpha uv}{1 + au} = 0, \end{cases} \tag{3.1}$$

from the first equation of Eq (3.1), we can obtain

$$v = \frac{1}{\beta}\left(r_1 + ar_1 u - Pr_1 u - aPr_1 u^2\right). \tag{3.2}$$

Substituting v in the second equation of Eq (3.1) with Eq (3.2), we obtain

$$h_0 u^4 + h_1 u^3 + h_2 u^2 + h_3 u + h_4 = 0, \tag{3.3}$$

where

$$h_0 = -\frac{a^2 P^2 Q r_1^2 r_2}{\beta^2}, h_1 = \frac{1}{\beta^2}\left(2a^2 PQ r_1^2 r_2 - 2aP^2 Q r_1^2 r_2\right),$$

$$h_2 = -\frac{1}{\beta}(\alpha Pr_1 + aPr_1 r_2) + \frac{1}{\beta^2}\left(4aPQ r_1^2 r_2 - a^2 Q r_1^2 r_2 - P^2 Q r_1^2 r_2\right),$$

$$h_3 = \frac{1}{\beta}(\alpha r_1 + ar_1 r_2 - Pr_1 r_2) + \frac{1}{\beta^2}\left(2PQ r_1^2 r_2 - 2aQ r_1^2 r_2\right), h_4 = \frac{r_1 r_2}{\beta} - \frac{Q r_1^2 r_2}{\beta^2}.$$

In the following discussion, we suppose that Eq (2.3) has a positive equilibrium (u_*, v_*).

In order to simplify discussions, we transform homogeneous state solution (u_*, v_*) into $(0, 0)$ by the means of transformation $(u, v) = (u_* + \tilde{u}, v_* + \tilde{v})$. We obtain

$$\begin{cases} f(\tilde{u}, \tilde{v}) = \left(r_1 + 2ar_1 u_* - 2Pr_1 u_* - 3aPr_1 {u_*}^2 - \beta v_*\right)\tilde{u} - \beta u_* \tilde{v} - aPr_1 \tilde{u}^3 \\ \qquad + (ar_1 - 3aPr_1 u_* - Pr_1)\,\tilde{u}^2 - \beta \tilde{u}\tilde{v} - aPr_1 u_*^3 + ar_1 u_*^2 - Pr_1 u_*^2 + r_1 u_* - \beta u_* v_*, \\ g(\tilde{u}, \tilde{v}) = (r_2 + ar_2 u_* - 2Qr_2 v_* - 2aQr_2 u_* v_* + \alpha u_*)\,\tilde{v} \\ \qquad + (ar_2 v_* - aQr_2 v_{*^2} + \alpha v_*)\,\tilde{u} + (-2aQr_2 v_* + ar_2 + \alpha)\,\tilde{u}\tilde{v} \\ \qquad + (-aQr_2 u_* - Qr_2)\,\tilde{v}^2 - aQr_2 u_* v_*^2 + ar_2 u_* v_* - Qr_2 v_*^2 + r_2 v_* + \alpha u_* v_*, \end{cases} \tag{3.4}$$

here and below, we call

$$\begin{aligned} a_1 &= r_1 + 2ar_1 u_* - 2Pr_1 u_* - 3aPr_1 u_{*^2} - \beta v_*, \\ a_2 &= r_2 + ar_2 u_* - 2Qr_2 v_* - 2aQr_2 u_* v_* + \alpha u_*, \\ b_1 &= \beta v_*, \\ b_2 &= ar_2 v_* - aQr_2 v_{*^2} + \alpha v_*, \\ e_1 &= -aPr_1 \tilde{u}^3 + (-3aPr_1 u_* + ar_1 - Pr_1)\,\tilde{u}^2 - \beta \tilde{u}\tilde{v} - aPr_1 u_*^3 + ar_1 u_*^2 \\ &\quad - Pr_1 u_*^2 + r_1 u_* - \beta u_* v_*, \\ e_2 &= +(-2aQr_2 v_* + ar_2 + \alpha)\,\tilde{u}\tilde{v} + (-aQr_2 u_* - Qr_2)\,\tilde{v}^2 - aQr_2 u_* v_*^2 \\ &\quad + ar_2 u_* v_* - Qr_2 v_*^2 + r_2 v_* + \alpha u_* v_*. \end{aligned}$$

Rewrite Eq (3.4) as follows

$$\begin{cases} f(\tilde{u},\tilde{v}) = a_1\tilde{u} - b_1\tilde{v} + e_1, \\ g(\tilde{u},\tilde{v}) = a_2\tilde{v} + b_2\tilde{u} + e_2. \end{cases}$$

Moreover, we explicitly incorporate length l into equations by transforming $x = l\tilde{x}$ and $y = l\tilde{y}$, which changes the domain $\Omega = [0,l]\times[0,l]$ to the unit square $\tilde{\Omega} = [0,1]\times[0,1]$, then Eq (2.3) become

$$\begin{cases} \dfrac{\partial\tilde{u}}{\partial t} = d_1\left(\dfrac{1}{l^2}\dfrac{\partial^2\tilde{u}}{\partial\tilde{x}^2} + \dfrac{1}{l^2}\dfrac{\partial^2\tilde{u}}{\partial\tilde{y}^2}\right) + a_1\tilde{u} - b_1\tilde{v} + e_1, \\ \dfrac{\partial\tilde{v}}{\partial t} = d_2\left(\dfrac{1}{l^2}\dfrac{\partial^2\tilde{v}}{\partial\tilde{x}^2} + \dfrac{1}{l^2}\dfrac{\partial^2\tilde{v}}{\partial\tilde{y}^2}\right) + a_2\tilde{v} + b_2\tilde{u} + e_2, \end{cases} \quad (\tilde{x},\tilde{y}) \in \tilde{\Omega} \tag{3.5}$$

with

$$\begin{cases} \tilde{u}(\tilde{x},\tilde{y},t) = u_0, \tilde{v}(\tilde{x},\tilde{y},t) = v_0, (\tilde{x},\tilde{y}) \in \partial\tilde{\Omega}, \\ f(u_0,v_0) = g(u_0,v_0) = 0. \end{cases} \tag{3.6}$$

For the sake of simplify and calculation, we express $\tilde{\Omega}$, $\tilde{x}$, $\tilde{y}$, and $\tilde{u}$, $\tilde{v}$ as Ω, x, y, and u, v.

Let

$$C_0^2(\Omega) := \left\{u \in C^2(\Omega); u|_{\partial\Omega} = 0\right\},$$

and

$$X := \left(C_0^2(\Omega)\right)^2, Y := (C(\Omega))^2,$$

we adapt Eq (3.5) as an operator equation

$$\frac{\partial \mathrm{U}}{\partial t} = \Phi(\mathrm{U}),$$

here $U := (u,v)$, and map $\Phi : X \to Y$ is defined as

$$\Phi(U) := \begin{pmatrix} \dfrac{d_1}{l^2}\dfrac{\partial^2 u}{\partial x^2} + \dfrac{d_1}{l^2}\dfrac{\partial^2 u}{\partial y^2} \\ \dfrac{d_2}{l^2}\dfrac{\partial^2 v}{\partial x^2} + \dfrac{d_2}{l^2}\dfrac{\partial^2 v}{\partial y^2} \end{pmatrix} + \begin{pmatrix} a_1u - b_1v + e_1 \\ a_2v + b_2u + e_2 \end{pmatrix}.$$

By differentiating U on homogeneous equilibrium solution $U_* \equiv (u_*,v_*) \equiv (0,0)$, we have the linearization of mapping Φ into L

$$\begin{aligned} L &:= D_u\Phi(U_*) \\ &= \begin{pmatrix} \dfrac{d_1}{l^2}\dfrac{\partial^2}{\partial x^2} + \dfrac{d_1}{l^2}\dfrac{\partial^2}{\partial y^2} & 0 \\ 0 & \dfrac{d_2}{l^2}\dfrac{\partial^2}{\partial x^2} + \dfrac{d_2}{l^2}\dfrac{\partial^2}{\partial y^2} \end{pmatrix} + \begin{pmatrix} a_1 & -b_1 \\ b_2 & a_2 \end{pmatrix}. \end{aligned}$$

The stability of U can be analyzed by the solution of variational problem

$$\frac{\partial U}{\partial t} = LU,$$

we decompose X in direct sum

$$X = \sum_{m,n=1}^{\infty} \oplus X_{m,n}, X_{m,n} := \left\{ \begin{pmatrix} c_1 \\ c_2 \end{pmatrix} \sin m\pi x \cdot \sin n\pi y; c_1, c_2 \in \mathbb{R} \right\}, m, n \in \mathbb{N}$$

and L maps $X_{m,n}$ to itself. Therefore,

$$\begin{aligned} & L \begin{pmatrix} c_1 \\ c_2 \end{pmatrix} \sin m\pi x \cdot \sin n\pi y \\ = & \begin{pmatrix} -d_1 \left(\frac{m^2}{l^2} + \frac{n^2}{l^2} \right) \pi^2 + a_1 & -b_1 \\ b_2 & -d_2 \left(\frac{m^2}{l^2} + \frac{n^2}{l^2} \right) \pi^2 + a_2 \end{pmatrix} \begin{pmatrix} c_1 \\ c_2 \end{pmatrix} \sin m\pi x \cdot \sin n\pi y. \end{aligned}$$

The limitation of L in subspace $X_{m,n}$ is a matrix of 2×2

$$\begin{aligned} & A_{m,n} := L \big|_{X_{m,n}} \\ = & \begin{pmatrix} -d_1 \left(\frac{m^2}{l^2} + \frac{n^2}{l^2} \right) \pi^2 + a_1 & -b_1 \\ b_2 & -d_2 \left(\frac{m^2}{l^2} + \frac{n^2}{l^2} \right) \pi^2 + a_2 \end{pmatrix}, m, n = 1, 2, \cdots . \end{aligned} \tag{3.7}$$

Therefore,

$$\text{Trace}\,(A_{m,n}) = -(d_1 + d_2) \left(\frac{m^2}{l^2} + \frac{n^2}{l^2} \right) \pi^2 + a_1 + a_2, \tag{3.8}$$

$$\text{Det}\,(A_{m,n}) = d_1 d_2 \left(\frac{m^2}{l^2} + \frac{n^2}{l^2} \right)^2 - (a_2 d_1 + a_1 d_2) \left(\frac{m^2}{l^2} + \frac{n^2}{l^2} \right) + a_1 a_2 + b_1 b_2. \tag{3.9}$$

4. Analysis of Turing instability and Hopf bifurcation

In this section, we mainly study the existence of Turing instability and Hopf bifurcation. We define a wave number k with $k^2 = m^2 + n^2 \in \mathbb{N}$, and denote $\theta = d_2/d_1$, $d_1 = d$, then the characteristic equation of $A_{m,n}$ is as follows:

$$\Lambda_k(\lambda, \theta) := \lambda^2 - \text{Trace}\,(k)\,\lambda + \text{Det}\,(k) = 0, k \in \mathbb{N}, \tag{4.1}$$

with

$$\text{Trace}\,(k) = -(1 + \theta) \frac{dk^2\pi^2}{l^2} + a_1 + a_2,$$

$$\text{Det}\,(k) = \theta \frac{d^2k^4\pi^4}{l^4} - (a_2 + a_1\theta) \frac{dk^2\pi^2}{l^2} + a_1 a_2 + b_1 b_2.$$

We assume that

(A_0) $-b_1 b_2/a_2 < a_1 < -a_2$.

(A_1) $0 < \theta < \theta_1, \theta_1 \triangleq \dfrac{a_1 a_2 + 2b_1 b_2}{a_1^2} - 2\sqrt{\dfrac{a_1 a_2 b_1 b_2 + b_1^2 b_2^2}{a_1^4}}$.

Under the assumption (A_0), all eigenvalues of $\Lambda_0(\lambda, \theta)$ have negative real parts, and Trace $(k) < 0$, for $k \in \mathbb{N}$.

Lemma 4.1. *Suppose that* (A_1) *holds, then* $\min_{k\in\mathbb{R}_+} \mathrm{Det}(k) < 0$.

Proof. Let $x = dk^2\pi^2/l^2 > 0$, then we rewrite Det (k) as

$$\begin{aligned} \mathrm{Det}(k) &= \theta x^2 - (a_2 + a_1\theta)\, x + a_1a_2 + b_1b_2 \\ &= \theta\left(x - \frac{a_2 + a_1\theta}{2\theta}\right)^2 + a_1a_2 + b_1b_2 - \frac{(a_2 + a_1\theta)^2}{4\theta}. \end{aligned} \tag{4.2}$$

From function (4.2), when $x = (a_2 + a_1\theta)/2\theta$, Det (k) can be taken to a minimum, that is, $\mathrm{Det}(k)_{min} = a_1a_2 + b_1b_2 - (a_2 + a_1\theta)^2/4\theta$. Since $x > 0$, we have $a_2 + a_1\theta > 0$. If we want $\mathrm{Det}(k)_{min} < 0$ with the condition $a_2 + a_1\theta > 0$, θ must satisfy $0 < \theta < (a_1a_2 + 2b_1b_2)/a_1^2 - 2\sqrt{\left(a_1a_2b_1b_2 + b_1^2b_2^2\right)/a_1^4}$. Hence, the lemma is proved. □

Let k_{min}^2 be the minimal point of function Det (k) on $k^2 \in \mathbb{R}_+$, then

$$k_{min} = \sqrt{\frac{l^2}{2d}\frac{a_2 + a_1\theta}{\theta\pi^2}}.$$

We make the following assumption to ensure $k_{min} > 0$

$(A_2)\ 0 < \theta < \theta_2(d), \theta_2(d) \triangleq \dfrac{a_2l^2}{\pi^2 d - a_1l^2}.$

$\theta = \theta_2(d)$ decreases monotonically in d and intersects with $\theta = \theta_1$ at the point $d = d_0$. Let $\theta_A(d) = \min_{d>0}\{\theta_1, \theta_2(d)\}$, then

$$\theta_A(d) = \begin{cases} \theta_1, 0 < d \le d_0, \\ \theta_2(d), d \ge d_0. \end{cases} \tag{4.3}$$

Hence, we have the following lemma.

Lemma 4.2. *Suppose that* (A_0) *holds, then assumptions* (A_1) *and* (A_2) *hold if and only if* $0 < \theta < \theta_A(d)$, $d > 0$.

4.1. Existence of Turing instability

4.1.1. Stability analysis of Turing instability

Denote

$$\theta_T(k, d) = \frac{\left(a_2dk^2\pi^2 - a_1a_2l^2 - b_1b_2l^2\right)l^2}{dk^2\pi^2\left(dk^2\pi^2 - a_1l^2\right)}, \quad \text{for } d > d_k, \tag{4.4}$$

where $d_k = \dfrac{(a_1a_2 + b_1b_2)\,l^2}{a_2k^2\pi^2}$, then Det $(k) = 0$ when $\theta = \theta_T(k, d)$.

Let $d_M(k)$ be the point at which monotonicity of function changes, that is, function $\theta = \theta_{\mathrm{T}}(k,d)$ increases monotonically if $d_k < d < d_M(k)$, and $\theta = \theta_{\mathrm{T}}(k,d)$ decreases monotonically if $d_M(k) < d < +\infty$. Hence, $\theta = \theta_{\mathrm{T}}(k,d)$ can take the maximum value θ_1 at $d_M(k)$.

Lemma 4.3. *Suppose that* (A_0) *holds, function* $\theta = \theta_{\mathrm{T}}(k,d)$ *has the following properties.*

(i) As for $k_i < k_{i+1}$, $k_i \in \mathbb{N}, i = 1,2,3\cdots$, *there is only one root* $d_{k_1,k_2} \in (d_M(k_2), d_M(k_1))$ *satisfies* $\theta_{\mathrm{T}}(k_1,d) = \theta_{\mathrm{T}}(k_2,d)$ *for* $d > 0$. *Furthermore,*

$$\theta_{\mathrm{T}}(k_1,d) > \theta_{\mathrm{T}}(k_2,d) > \theta_{\mathrm{T}}(k_3,d) > \cdots, \text{for} \quad d > d_{k_i,k_{i+1}}.$$

(ii) Define $d_{0,k_1} = +\infty$, *and*

$$\theta_{\mathrm{T}} \triangleq \theta_{\mathrm{T}}(d) = \theta_{\mathrm{T}}(k,d), d \in (d_{k_{i+1},k_{i+2}}, d_{k_i,k_{i+1}}), k_i \in \mathbb{N}, i = 1,2,3\cdots.$$

Then

$$\theta_{\mathrm{T}}(d) \le \theta_A(d), 0 < d < +\infty.$$

Moreover, $\theta_{\mathrm{T}}(d) = \theta_{\mathrm{A}}(d)$ *if and only if* $d = d_M(k)$, $k \in \mathbb{N}$.

We display the relation between $\theta = \theta_1$, $\theta = \theta_2(d)$ and $\theta = \theta_{\mathrm{T}}(k,d)$ in Figure 1, where $d > 0$, $k = 5, 10, 13\cdots$.

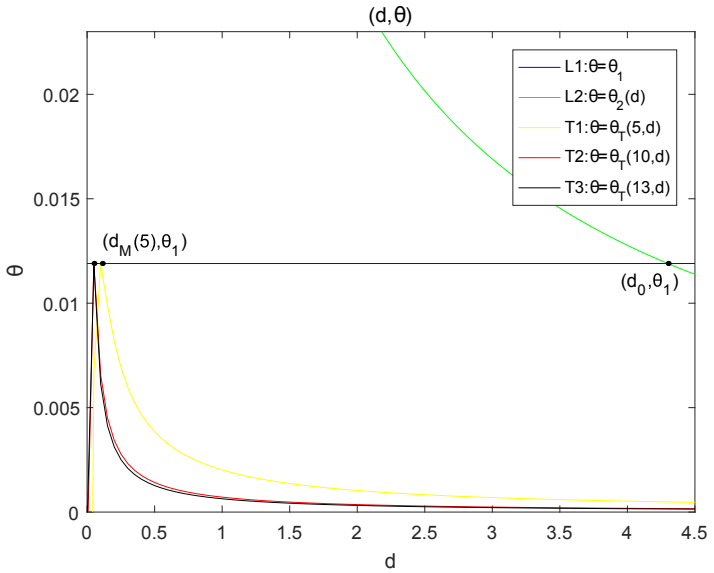

Figure 1. The figure of functions $\theta = \theta_1$, $\theta = \theta_2(d)$ and $\theta = \theta_{\mathrm{T}}(k,d)$, $d > 0$, $k = 5, 10, 13\cdots$, in (d,θ) plane.

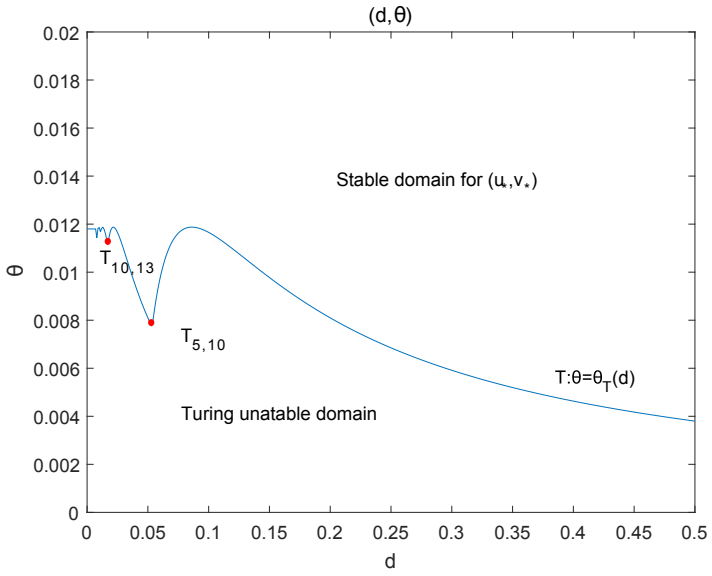

Figure 2. The Turing bifurcation line $T : \theta = \theta_T(d)$, $d > 0$.

Theorem 4.1. *Suppose that* (A_0) *holds.*
(1) For any given $k_1 \in \mathbb{N}$, *when* $\theta = \theta_T(k_1, d)$, *system (3.5) occurs Turing bifurcation at* (u_*, v_*).
(2) $\theta = \theta_T(d)$, $d > 0$ *is the critical curve of Turing instability.*
(i) If $\theta > \theta_T(d)$, $d > 0$, *system (3.5) is asymptotically stable at* (u_*, v_*).
(ii) If $0 < \theta < \theta_T(d)$, $d > 0$, *Turing instability occurs in system (3.5) at* (u_*, v_*).

Proof. When $\theta = \theta_T(k_1, d)$, we have $\mathrm{Det}(k_1) = 0$. Then Eq (4.1) becomes

$$\Lambda_{k_1}(\lambda, \theta) := \lambda^2 - \mathrm{Trace}(k_1)\lambda = 0. \tag{4.5}$$

The Eq (4.5) has a zero root, and the other root of $\Lambda_{k_1}(\lambda, \theta)$ has negative real part. That is, Eq (3.5) occurs Turing bifurcation at (u_*, v_*) when $\theta = \theta_T(k_1, d)$.

When $\theta > \theta_T(d)$, $d > 0$, $\mathrm{Det}(k_1) > 0$. (A_0) ensures that $\mathrm{Trace}(k_1) < 0$, then all roots of $\Lambda_{k_1}(\lambda, \theta)$ have negative real parts. On the other hand, when $0 < \theta < \theta_T(d)$, $d > 0$, $\mathrm{Det}(k_1) < 0$, so system (3.5) is Turing instability. □

Remark 4.1. *When* $\theta > \theta_T(d)$, $d > 0$, *system (3.5) occurs steady-state bifurcation at positive equilibrium* (u_*, v_*).
(1) If $m = n$, *the bifurcation type is a simple steady-state bifurcation.*
(2) If $m \neq n$, *the bifurcation type is a double steady-state bifurcation.*

4.1.2. Numerical simulations of Turing bifurcation

Let $r_1 = 1$, $r_2 = 0.01$, $P = 10$, $Q = 20$, $a = 0.01$, $\alpha = 8$, $\beta = 11$, $l = 3$, we obtain positive equilibrium of system (2.3) is

$$(u_*, v_*) = (0.01, 0.0818),$$

and $a_1 = -0.0996$, $a_2 = 0.0573$, $b_1 = 0.11$, $b_2 = 0.6544$. Through (A_1), (A_2), Eqs (4.3,4.4), we obtain $\theta_1 = 0.0119$,

$$\theta_A(d) = \begin{cases} 0.0119, & 0 < d \leq 4.3, \\ \dfrac{0.5157}{d\pi^2 + 0.8964}, & d \geq 4.3, \end{cases}$$

and

$$\theta_T(k_1, d) = \frac{-5.3703 + 0.5157dk_1^2\pi^2}{dk_1^2\pi^2\left(dk_1^2\pi^2 + 0.8964\right)}.$$

By setting $k_1 = 5$, $m_1 = 3$, $n_1 = 4$, we obtain $d_{0,5} = +\infty$ and $d_{5,10} = 0.0535$. Select $d = d_1 = 0.06 \in [d_{5,10}, d_{0,5})$, thus $\theta_T = \theta_T(5, 0.06) = 0.0097$. Equation (3.5) with $d = 0.06$ undergoes Turing bifurcation near equilibrium $(0.01, 0.0818)$ at $\theta = 0.0097$. Since $m_1 \neq n_1$, that is, the bifurcation type of Eq (3.5) is double steady-state bifurcation, and we derive the following mixed patterns.

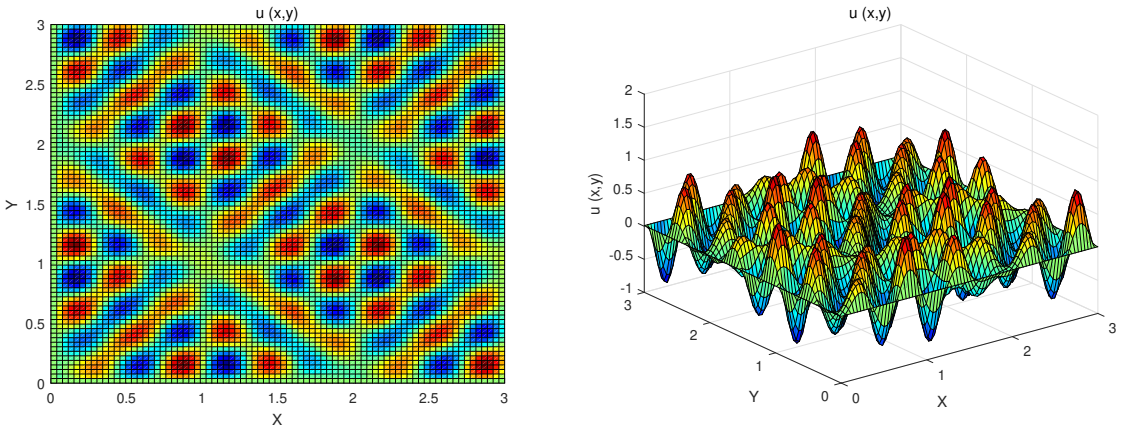

Figure 3. X-Y-U mixed pattern under the condition of $m_1 = 3$, $n_1 = 4$.

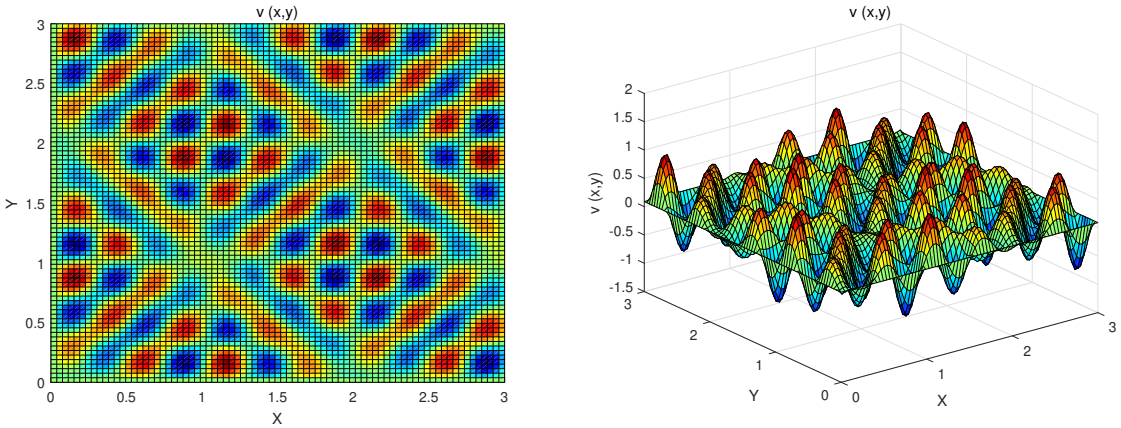

Figure 4. X-Y-V mixed pattern under the condition of $m_1 = 3$, $n_1 = 4$.

4.2. Existence of Hopf bifurcation

4.2.1. Stability analysis of Hopf bifurcation

We assume that
$(A_0)^{'}$ $a_1 > max\{-a_2, -b_1 b_2/a_2\}$.

Denote

$$\theta_H(k,d) = \frac{(a_1+a_2)\,l^2 - dk^2\pi^2}{dk^2\pi^2}, \quad \text{for } 0 < d < d_k, \tag{4.6}$$

where $d_k = \dfrac{(a_1+a_2)\,l^2}{k^2\pi^2}$, then $\mathrm{Trace}(k) = 0$ when $\theta = \theta_H(k,d)$.

$\theta = \theta_H(k,d)$ decreases monotonically in d and intersects with $\theta = \theta_1$ at the point $d = d_H$. On the basis of Lemma 4.1, it is known that $\min\limits_{k\in\mathbb{R}_+} \mathrm{Det}(k) < 0$ if $0 < \theta < \theta_1$, then we obtain the following theorem.

Theorem 4.2. *Suppose that* $(A_0)^{'}$ *holds. For any given* $k_1 \in \mathbb{N}$, *when* $\theta = \theta_H(k_1,d) > \theta_1$, $0 < d < d_H$, *system (3.5) occurs Hopf bifurcation at positive equilibrium* (u_*, v_*).

Proof. $\theta = \theta_H(k_1,d)$, we have $\mathrm{Trace}(k_1) = 0$, then Eq (4.1) becomes

$$\Lambda_{k_1}(\lambda,\theta) := \lambda^2 + \mathrm{Det}(k_1) = 0. \tag{4.7}$$

Since $\theta > \theta_1$, through assumption $(A_0)^{'}$, $\mathrm{Det}(k_1) > 0$, we know that Eq (4.7) has a pair of pure imaginary roots. The above satisfies conditions for the generation of Hopf bifurcation. □

4.2.2. Numerical simulations of Hopf bifurcation

Let $r_1 = 1$, $r_2 = 0.01$, $P = 1$, $Q = 10$, $a = 0.01$, $\alpha = 8$, $\beta = 8$, $l = 3$, we can solve positive equilibrium of Eq (2.3) to obtain

$$(u_*, v_*) = (0.003, 0.125).$$

We then obtain $a_1 = -0.0059$, $a_2 = 0.009$, $b_1 = 0.024$, $b_2 = 1$. Through assumption (A_1) and (4.6), we have $\theta_1 = 0.0008$, and

$$\theta_H(k,d) = \frac{0.0279 - dk^2\pi^2}{dk^2\pi^2}.$$

By setting $m_3 = 5$, $n_3 = 12$, we obtain $d_H = 1.6714 \times 10^{-5}$. We choose $d = 1.5206 \times 10^{-5}$ which is satisfied $d < d_H$, and obtain $\theta_H = 0.1$. The relationship between $\theta = \theta_1$ and $\theta = \theta_H(k,d)$ can be reflected by Figure 5.

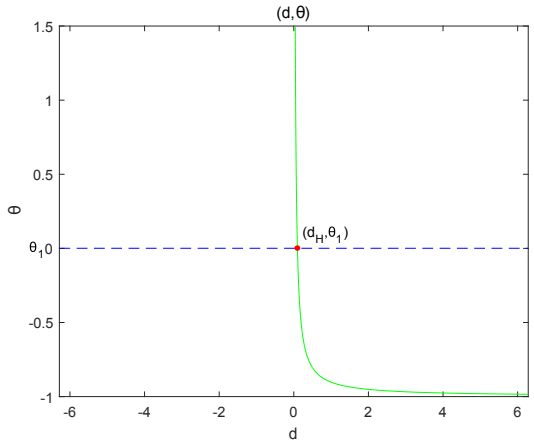

Figure 5. The figure of functions $\theta = \theta_1$ and $\theta = \theta_{\mathrm{H}}\,(k, d)$ in (d, θ) plane.

Hopf bifurcation occurs at $\theta = 0.1$, we can obtain hyperhexagonal patterns in Figures 6 and 7.

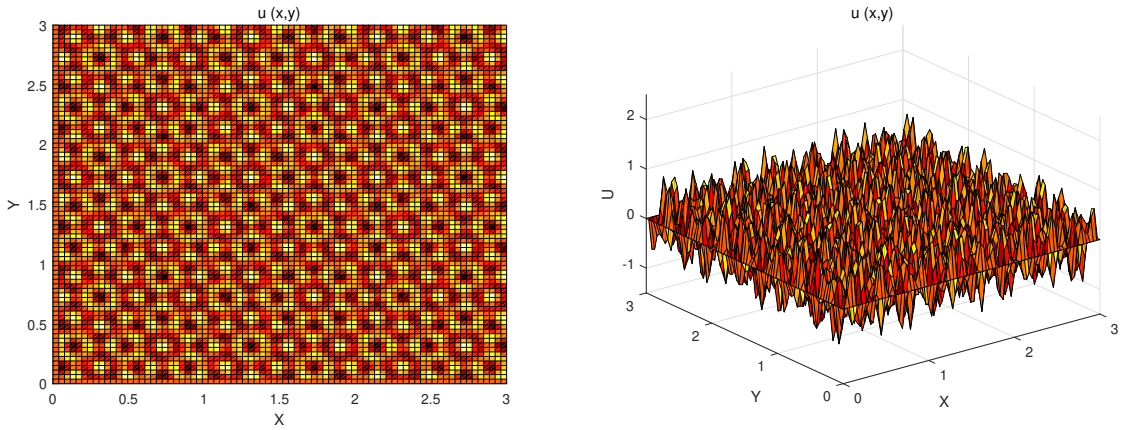

Figure 6. X-Y-U hyperhexagonal pattern under the condition of $m_3 = 5$, $n_3 = 12$.

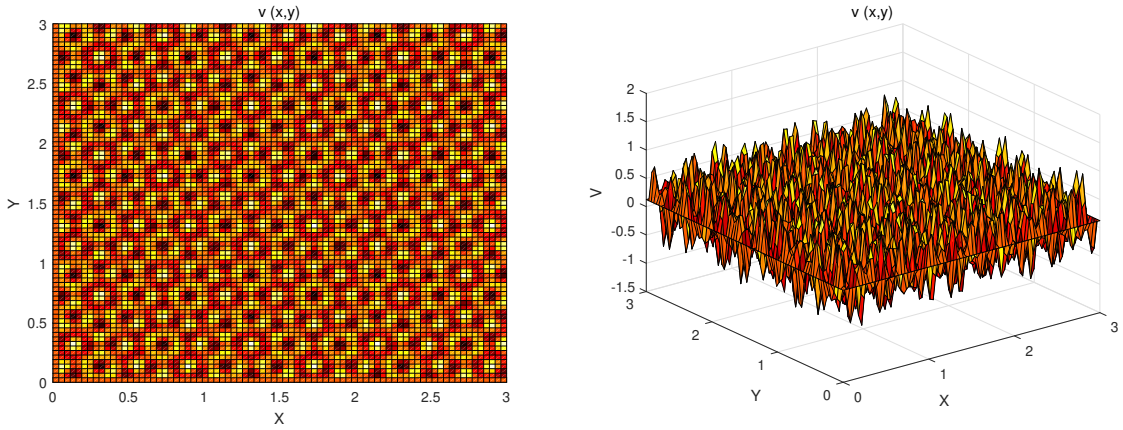

Figure 7. X-Y-V hyperhexagonal pattern under the condition of $m_3 = 5$, $n_3 = 12$.

Moreover, from Figures 8 and 9, we observe that $u(x,t)$ and $v(x,t)$ are periodic in relation to t, that is, there is a stable bifurcation periodic solution near the positive equilibrium of Eq (2.3).

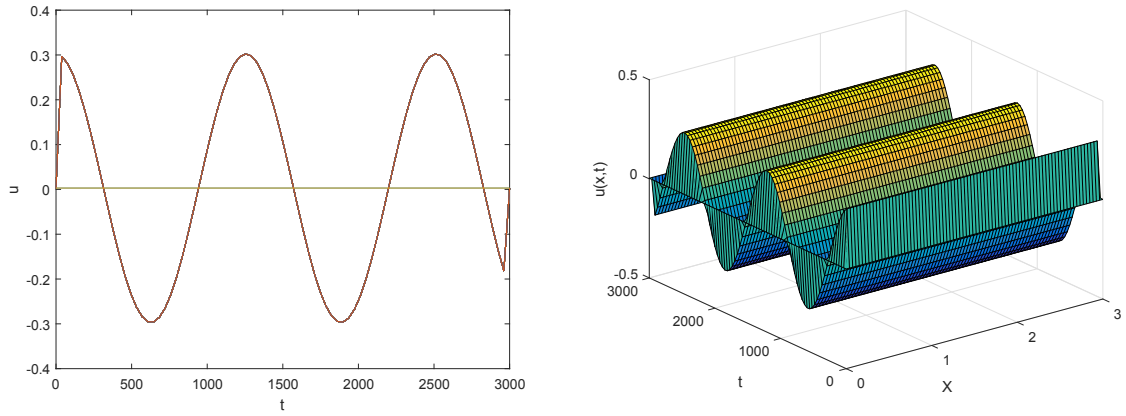

Figure 8. $u(x,t)$ periodic solution image.

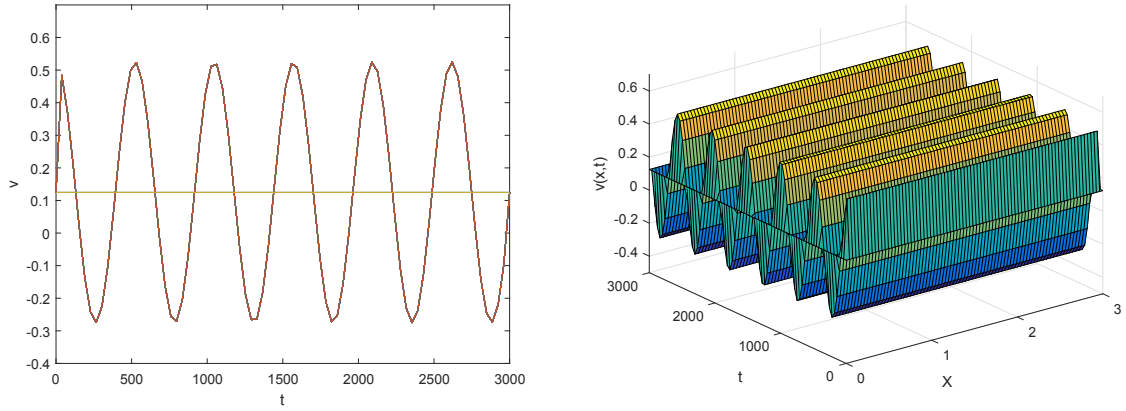

Figure 9. $v(x,t)$ periodic solution image.

5. Conclusions

DLG system to model forest recovery as the spread of land-cover classes in continuous space and time. However, there is only one variable u in DLG system. In this paper, we establish a reaction diffusion model based on DLG system and Holling II functional responses, we can use this model to reflect the variable relationship between forest restoration and population pressure. When the population pressure increases, the density of forest restoration will decrease. On the contrary, when the population pressure decreases, the density of forest restoration will increase and the situation of forest restoration will be improved. We also consider the effect of population pressure on forest restoration, through Eq (2.3).

Under Dirichlet boundary conditions, we obtain a positive equilibrium. According to linear stability analysis of positive equilibrium solution of Eq (3.5) and discussion of eigenvalue attributes of the

matrix, we obtain the conditions for Turing instability and Hopf bifurcation. Furthermore, the steady-state bifurcation is divided into simple steady-state bifurcation and double steady-state bifurcation. In addition, we verify the existence of Turing instability and Hopf bifurcation by numerical simulation, and obtain different kinds of patterns.

Our work is to further study the diffusion logistic growth (DLG) model, which helps ease the relationship between forest restoration and population pressure.

Acknowledgments

This research is supported by the Fundamental Research Funds for the Central Universities (2572017BB03) and Science and Technology Innovation Talent Research Fund of Harbin (2017RAQXJ108). The authors wish to express their gratitude to the editors and the reviewers for the helpful comments.

Conflict of Interests

The authors declare there is no conflict of interest

References

1. R. Brown, J. Agee, J. F. Franklin, Forest restoration and fire: principles in the context of place, *Conserv. Biol.*, **18** (2004), 903–912.
2. C. Ravenscroft, R. Scheller, D. Mladenoff, M. A. White, Forest restoration in a mixed-ownership landscape under climate change, *Ecol. Appl.*, **20** (2010), 327–346.
3. H. Bateman, D. Merritt, J. Johnson, Riparian forest restoration: Conflicting goals, trade-offs, and measures of success, *Sustainability*, **4** (2012), 2334–2347.
4. S. Peng, Y. Hou, B. Chen, Establishment of Markov successional model and its application for forest restoration reference in Southern China, *Ecol. Modell.*, **221** (2010), 1317–1324.
5. T. Aide, J. Cavelier, Barriers to lowland tropical forest restoration in the Sierra Nevada de Santa Marta, Colombia, *Restor. Ecol.*, **2** (1994), 219–229.
6. R. Chazdon, Tropical forest recovery: Legacies of human impact and natural disturbances, *Perspect. Plant Ecol. Evol. Syst.*, **6** (2003), 51–71.
7. A. Okubo, *Diffusion and Ecological Problems: Mathematical Models*, Springer Verlag, New York, (1980).
8. C. Zhang, A. Ke, B. Zheng, Patterns of interaction of coupled reaction-diffusion systems of the FitzHugh-Nagumo type, *Nonlinear Dyn.*, **97** (2019), 1451–1476.
9. K. Jesse, Modelling of a diffusive Lotka-Volterra-System: The climate-induced shifting of tundra and forest realms in North-America, *Ecol. Modell.*, **123** (1999), 53–64.
10. Y. Svirezhev, Lotka-Volterra models and the global vegetation pattern, *Ecol. Modell.*, **135** (2000), 135–146.

11. M. Acevedo, M. Marcano M, R. Fletcher, A diffusive logistic growth model to describe forest recovery, *Ecol. Modell.*, **244** (2012), 13–19.
12. E. Holmes, M. Lewis, J. Banks, R. R. Veit, Partial differential equations in ecology: Spatial interactions and population dynamics, *Ecology*, **75** (1994), 17–29.
13. P. Vitousek, Beyond global warming: Ecology and global change, *Ecology*, **75** (1994), 1861–1876.
14. C. Nunes, J. Auge, *Land-use and Land-cover Change (LUCC): Implementation Strategy*, International Geosphere-Biosphere Programme, Environmental Policy Collection, 1999.
15. T. Houet, P. Verburg, T. Loveland, Monitoring and modelling landscape dynamics, *Landscape Ecol.*, **25** (2010), 163–167.
16. H. Pereira, P. Leadley, V. Proença, R. Alkemade, J. P. W. Scharlemann, J. F. Fernandez-Manjarres, et al., Scenarios for global biodiversity in the 21st century, *Science*, **330** (2010), 1496–1501.
17. T. Chase, R. Pielke, T. Kittel, R. R. Nemani, S. W. Running, Simulated impacts of historical land cover changes on global climate in northern winter, *Clim. Dyn.*, **16** (2000), 93–105.
18. R. Houghton, J. Hackler, K. Lawrence, The US carbon budget: contributions from land-use change, *Science*, **285** (1999), 574–578.
19. E. Lambin, B. Turner, H. Geist, S. B.Agbola, A. Angelsen, J. W. Brucee, et al., The causes of land-use and land-cover change: Moving beyond the myths, *Global Environ. Change*, **11** (2001), 261–269.
20. R. Chazdon, M. Guariguata, Natural regeneration as a tool for large-scale forest restoration in the tropics: Prospects and challenges, *Biotropica*, **48** (2016), 716–730.
21. T. Crk, M. Uriarte, F. Corsi, D. Flynn, Forest recovery in a tropical landscape: What is the relative importance of biophysical, socioeconomic, and landscape variables?, *Landscape Ecol.*, **24** (2009), 629–642.
22. J. Chinea, Tropical forest succession on abandoned farms in the Humacao Municipality of eastern Puerto Rico, *For. Ecol. Manage.*, **167** (2002), 195–207.
23. C. Chien, M. Chen, Multiple bifurcations in a reaction-diffusion problem, *Comput. Math. Appl.*, **35** (1998), 15–39.
24. W. Jiang, H. Wang, X. Cao, Turing instability and Turing-Hopf bifurcation in diffusive Schnakenberg systems with gene expression time delay, *J. Dyn. Differ. Equations*, **31** (2019), 2223–2247.
25. R. Fisher, The wave of advance of advantageous genes, *Ann. Hum. Genet.*, **7** (1937), 355–369.
26. Z. Ju, Y. Shao, W. Kong, X. Ma, X. Fang, An impulsive prey-predator system with stage-structure and Holling II functional response, *Adv. Differ. Equations*, **2014** (2014), 280.
27. S. Madec, J. Casas, G. Barles, C. Suppo, Bistability induced by generalist natural enemies can reverse pest invasions, *J. Math. Biol.*, **75** (2017), 543–575.